

**$B(E2)$  values and phase coexistence in  $^{152}\text{Sm}$** N. V. Zamfir,<sup>1,2</sup> R. F. Casten,<sup>1</sup> M. A. Caprio,<sup>1</sup> C. W. Beausang,<sup>1</sup> R. Krücken,<sup>1</sup> J. R. Novak,<sup>1</sup> J. R. Cooper,<sup>1</sup>  
G. Cata-Danil,<sup>1,3</sup> and C. J. Barton<sup>2</sup><sup>1</sup>*Wright Nuclear Structure Laboratory, Yale University, New Haven, Connecticut 06520*<sup>2</sup>*Clark University, Worcester, Massachusetts 01610*<sup>3</sup>*National Institute for Physics and Nuclear Engineering, Bucharest-Magurele, Romania*

(Received 13 May 1999; published 4 October 1999)

The  $B(E2)$  values for several critical transitions in  $^{152}\text{Sm}$  are determined following the  $\epsilon$  decay of  $^{152}\text{Eu}$ . These data improve upon and correct previous studies and allow us to perform a full analysis of phase coexistence in  $^{152}\text{Sm}$ , to analyze the mixing found empirically, and to compare this with detailed model calculations. [S0556-2813(99)06510-3]

PACS number(s): 21.10.-k, 21.60.Ev, 23.20.-g, 27.70.+q

**I. INTRODUCTION**

In two recent papers [1,2] evidence for phase coexistence in  $^{152}\text{Sm}$  was presented. In a third paper [3], evidence for a corresponding phase transition in the  $A \sim 150$  mass region was studied.

The results are of particular interest because they relate to phase coexistence (in the sense of condensed matter or magnetic systems) stemming from a single Hilbert space [2]. Of course, since nuclei are finite systems, the concepts of phase transitions and coexistence are only approximate. The ideas in Refs. [1–3] can be visualized in terms of two coexisting potentials, spherical and deformed, whose energy separation varies with nucleon number such that  $^{152}\text{Sm}$  is near the crossing point and shows evidence for both types of structure at low energies. Such a level crossing scenario is closely related to the concept of a first-order phase transition although, in the finite-body nuclear case, the abruptness of such a structural change is naturally muted.

We stress that the phenomena involved here are quite distinct from other widespread and familiar types of *shape* coexistence that involve the mechanism of an intruder state from another major shell. (This is not to say that the energy and interaction of the  $\nu 1h_{9/2}$  orbit and its spin orbit partner  $\pi 1h_{11/2}$  are unimportant for understanding the transition region. However, the onset of deformation nevertheless arises from effects within single proton and neutron major shells.) Model analyses suggest that this kind of phase coexistence corresponds to only a small region of parameter space and is therefore likely to be an extremely rare phenomenon.

A simplified view of the  $^{152}\text{Sm}$  level scheme is shown in Fig. 1 (left). In the coexistence interpretation the yrast levels constitute a deformed rotational band [ $R_{4/2}^{(1)} \equiv E(4_1^+)/E(2_1^+) = 3.01$ ] while the states built on the  $0_2^+$  level comprise a vibrational sequence of phonon and multiphonon levels ( $R_{4/2}^{(2)} \equiv [E(4_2^+) - E(0_2^+)]/[E(2_2^+) - E(0_2^+)] = 2.69$ ). In this view, for example, the  $2_2^+$  level would be a 1-phonon excitation of the  $0_2^+$  level and the  $4_2^+$ ,  $2_3^+$ , and  $0_3^+$  levels would be the 2-phonon excitations. The coexistence interpretation was motivated by and centered on the observations of the low value of  $R_{4/2}^{(2)}$  and of an extremely weak  $B(E2: 2_3^+ \rightarrow 0_2^+)$  value [1] of  $\sim 0.17$  W.u.: this transition is forbidden because it requires the destruction of two phonons, whereas

in either a purely rotational or purely spherical vibrational interpretation of  $^{152}\text{Sm}$  the  $2_3^+ \rightarrow 0_2^+$  transition is expected to be collective. Coexisting  $0^+$  states are also supported by data from  $(p, t)$  and  $(t, p)$  cross sections to  $0^+$  states in  $^{152}\text{Sm}$  (see, for example, Ref. [4]). The levels based on the  $0_2^+$  state clearly resemble a set of phonon and multiphonon levels. In fact, the yrast and near yrast levels built on the  $0_2^+$  state, if taken in isolation (e.g., if one encountered a nucleus where the  $0_2^+$  level was the ground state) would be almost a textbook example of an anharmonic vibrator spectrum. This is illustrated in Fig. 1 where we compare the experimental levels of the  $0_2^+$ -sequence to anharmonic vibrator model calculations obtained with the equivalent approaches of Brink *et al.* [5] or of the U(5) limit of the interacting boson approximation (IBA). We have used only a single anharmonicity parameter for all states, chosen to reproduce the two-phonon  $4^+$  energy. This figure vividly shows the phonon multiplets and very closely resembles the data. Such a sequence of levels, with such uniformity, is unexpected in *any* nucleus much less as a coexisting family of excited states. Indeed, only in the Cd isotopes [6–9] are candidates for 4 (and maybe) 5 phonon vibrational states (built on the ground state) known at all.

However, this picture of  $^{152}\text{Sm}$  faces a number of serious difficulties and puzzles based on the existing data, especially when absolute transition rates are considered. There are several key issues that can be summarized as follows (most of these are illustrated on the left in Fig. 2).

(1) The very small  $B(E2)$  value for the 401 keV  $2_3^+ \rightarrow 0_2^+$  transition itself. This value was not actually definitively established in Ref. [1]. It was remarked in Ref. [1] that the value obtained should be considered as an upper limit since the 401 keV transition in the spectrum could be partly a contaminant. ( $^{154}\text{Eu}$  is  $\beta$  unstable and also has a 401 keV transition.)

(2) The  $B(E2)$  value for the 126 keV  $2_2^+ \rightarrow 0_2^+$  transition presents a major problem. The Nuclear Data Sheets (NDS) [10] have adopted an enormous  $B(E2)$  value of 520(170) W.u., stemming from the data in Ref. [11]. This value would be 3.6 times the  $B(E2: 2_1^+ \rightarrow 0_1^+)$  value of 144 W.u. and therefore almost impossible to understand. Indeed, it would be larger than any  $B(E2: 2_1^+ \rightarrow 0_1^+)$  value known. In a deformed nucleus, the  $2_2^+$  level would be a rotational excitation

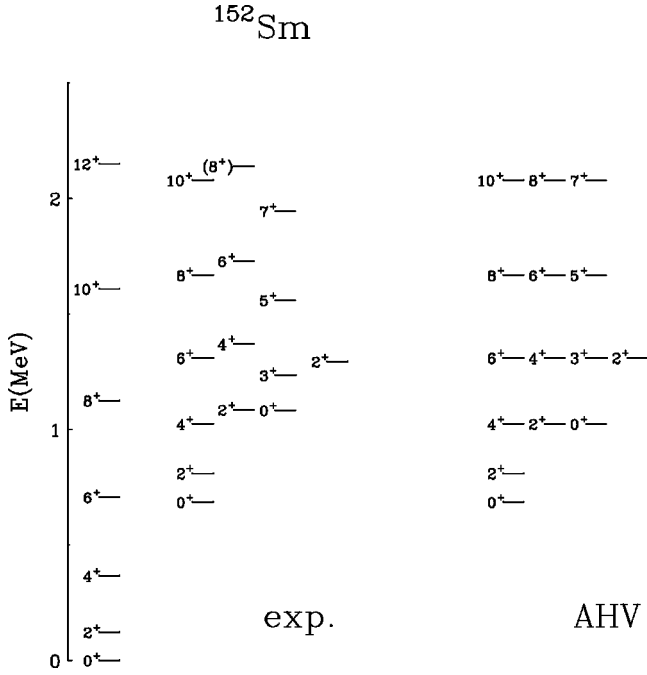


FIG. 1. Empirical levels of  $^{152}\text{Sm}$  (left). The experimental levels built on the  $0_2^+$  level are compared with those predicted for an anharmonic vibrator (AHV) on the right.

of the  $K=0_2^+$  bandhead and should have a  $B(E2: 2_2^+ \rightarrow 0_2^+)$  value comparable to the  $B(E2: 2_1^+ \rightarrow 0_1^+)$  value of 144 W.u. In a vibrational picture, or in any intermediate or transitional structure, it is even more difficult to envision a  $B(E2: 2_2^+ \rightarrow 0_2^+)$  value anywhere near 520 W.u.

A harmonic vibrator description of the levels built on the  $0_2^+$  state implies certain relations among the  $B(E2)$  values between these levels and to the yrast states. Particular problems therefore are as follows.

(3) The reported [10]  $M1$  nature of the 275 keV  $2_3^+ \rightarrow 2_2^+$  transition. In the vibrator picture for the  $0_2^+$ -based levels, the  $2_3^+$  level, as noted above, should be a two phonon

excitation of the  $0_2^+$  state and therefore [given the strong  $B(E2: 2_2^+ \rightarrow 0_2^+)$  value] should have a large  $B(E2)$  value to the  $2_2^+$  state.

(4) The contrast of this  $M1$  transition with the extremely strong  $B(E2)$  value for the 213 keV  $4_2^+ \rightarrow 2_2^+$  transition. If both the  $2_3^+$  and  $4_2^+$  levels are 2-phonon states they should have similar  $B(E2)$  values to the  $2_2^+$  state. However, as we just pointed out, no  $B(E2)$  content is known in the  $2_3^+ \rightarrow 2_2^+$  transition, whereas the  $B(E2: 4_2^+ \rightarrow 2_2^+)$  value is given in Ref. [10] as  $\approx 400$  W.u. Though this value, based on a Coulomb excitation analysis in Ref. [12], has a large uncertainty, as stated in Ref. [12] itself, its contrast with the lack of any  $E2$  transition from the  $2_3^+$  to the  $2_2^+$  level is completely inconsistent with a vibrator picture. Note that, even if the  $2_3^+ \rightarrow 2_2^+$  transition were actually  $E2$ , its  $B(E2)$  value would only be  $\sim 13$  W.u., far from the value of 400 W.u. for the  $4_2^+ \rightarrow 2_2^+$  transition.

(5) The weak  $B(E2)$  values for the 349 keV and 286 keV  $4_3^+ \rightarrow 4_2^+$  and  $4_3^+ \rightarrow 2_3^+$  transitions, respectively. The  $4_3^+$  level in the vibrator interpretation is a 3-phonon excitation of the  $0_2^+$  level and should have large  $B(E2)$  values to the two-phonon  $4_2^+$  and  $2_3^+$  levels. These  $B(E2)$  values should be stronger than the value for the  $2_2^+ \rightarrow 0_2^+$  value. Yet, experimentally, the  $4_3^+ \rightarrow 4_2^+$  transition has not been seen and the  $B(E2)$  value for the  $4_3^+ \rightarrow 2_3^+$  transition is only 50 W.u.

(6) Crossover transitions from the  $0_2^+$ -based levels of the vibrator sequence into the ground-state band. In a strict scenario of distinct rotor and vibrator level sequences, crossover transitions would vanish. Yet, two of these transitions are collective ( $\sim 20$ – $30$  W.u.) while the others are quite weak (a few W.u.). Therefore, one needs to understand the origin of the two collective branches, and also understand why the others are weak. One can guess that the crossover transitions arise from mixing between the two level sequences but this needs to be accounted for quantitatively in a way that is consistent with the full body of data in  $^{152}\text{Sm}$ .

(7) The energy spacing, 126 keV, between the  $2_2^+$  and  $0_2^+$  levels. This spacing is almost exactly the same as the  $2_1^+ - 0_1^+$  energy difference of 122 keV, which would seem unlikely if these states have structures as different as vibrational and rotational, respectively.

The purpose of this paper is to report on an experiment that used the high efficiency of the YRAST Ball array [13] at WNSL at Yale to obtain absolute  $B(E2)$  values for the critical transitions listed and discussed above by measuring  $\gamma$ -ray intensities and branching ratios and using known level half-lives. After presenting the experimental results we will further analyze the  $^{152}\text{Sm}$  level scheme and present a more complete and extensive discussion of its structure. Our discussion will include a model independent treatment of the mixing of the low-lying states and detailed IBA model predictions as well. This will lead to a more complete understanding of the phase coexistence interpretation and of the nature of the anharmonic vibrational states built on the  $0_2^+$  level, and will point toward some dissolution of vibrational structure for certain levels built on the  $0_2^+$  state.

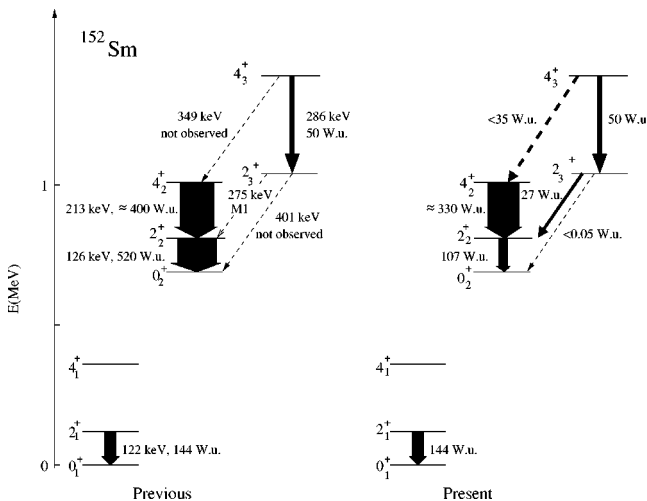


FIG. 2. Partial level scheme for  $^{152}\text{Sm}$  highlighting the differences between previously adopted results (left) [10] and those from the present work (right).

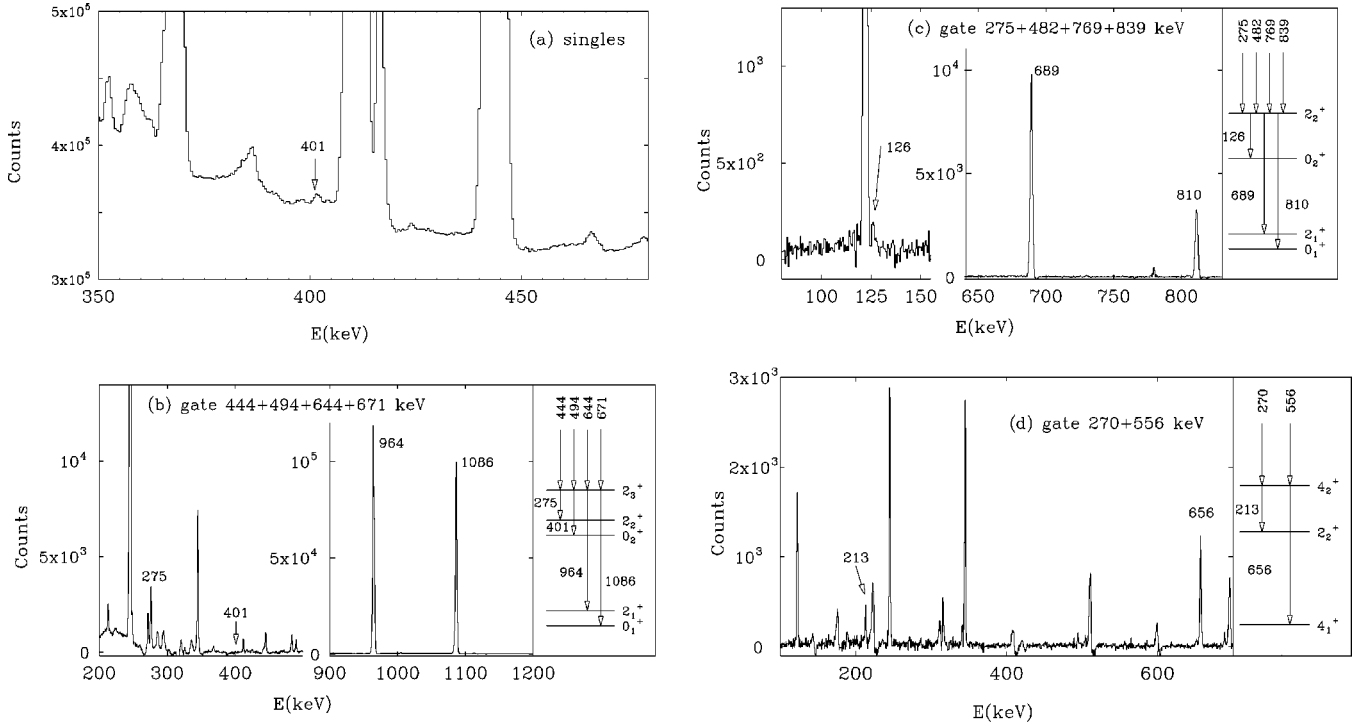


FIG. 3. Gamma-ray data from the present measurements. (a) Singles spectrum; (b), (c), and (d) key coincidence spectra. The partial level schemes at the right illustrate the gates and the essential coincidence relations revealed in these spectra.

**II. EXPERIMENTAL RESULTS**

As with the original experiment presented in Ref. [1], the current study measured  $\gamma$  transitions following the  $\epsilon$  decay of  $^{152}\text{Eu}$ . A standard  $^{152}\text{Eu}$  source was mounted at the center of the detector array YRAST Ball, and both single and  $\gamma\gamma$  coincidence events were recorded. The source strength was  $7\mu\text{Ci}$ , the counting time 25 days, and the total YRAST Ball photopeak efficiency was 1.7% at 1.3 MeV in a configuration

that included three segmented Clover detectors, one 70% detector, 16 normal medium efficiency ( $\sim 25\%$ ) and one LEPS detector, each at a distance (source to detector face) of 20 cm. All detectors were Compton suppressed with either BGO or NaI except for the LEPS detector.

An example of the singles data in the region of the 401 keV  $2_3^+ \rightarrow 0_2^+$  transition is shown in Fig. 3(a), while selected coincidence gates relevant to the discussion below are shown in Figs. 3(b)–(d). We now discuss the key new results in

TABLE I. Intensities and  $B(E2)$  values obtained in the present work.

$J_i \rightarrow J_{f1}$	$I(J_i \rightarrow J_{f1})$	$I(J_i \rightarrow J_{f2})$	$B(E2 : J_i \rightarrow J_{f2})(\text{W.u.})^a$	$E_\gamma(J_i \rightarrow J_{f1})$	$B(E2 : J_i \rightarrow J_{f1})(\text{W.u.})^b$
$2_3 \rightarrow 0_2$	$\leq 0.0002$		3.62(17)	401 keV	$\leq 0.05$
$2_3 \rightarrow 0_1$					
$2_2 \rightarrow 0_2$	0.004(1)		5.5(5)	126 keV	107(27)
$2_2 \rightarrow 2_1$					
$2_3 \rightarrow 2_2$	0.008(1)		3.62(17)	275 keV	27(4)
$2_3 \rightarrow 0_1$					
$4_2 \rightarrow 2_2$	0.11(1)		$\approx 9$	213 keV	$\approx 330$
$4_2 \rightarrow 4_1$					
$4_3 \rightarrow 4_2$	$\leq 0.03$		5.5(16)	349 keV	$\leq 35$
$4_3 \rightarrow 4_1$					
$4_3 \rightarrow 3_1$	$\leq 0.002$		5.5(16)	138 keV	$\leq 250$
$4_3 \rightarrow 4_1$					
$2_4 \rightarrow 0_2$	$\leq 1.0$		$> 0.45$	608 keV	
$2_4 \rightarrow 4_1$					

<sup>a</sup>From Ref. [8].

<sup>b</sup>Deduced from the data in the columns to the left.

terms of these spectra. The present results are summarized in Table I and on the right in Fig. 2.

Comparison of the singles data in Fig. 3(a) with the corresponding Fig. 1 of Ref. [1] shows that the present results have comparable energy resolution, about 20 times better statistics, and apparent evidence for the 401 keV peak. However, careful inspection of the full  $\gamma$ -ray spectrum shows lines from a  $^{154}\text{Eu}$  contaminant. When these are properly subtracted essentially all of the singles intensity of the 401 keV transition in  $^{152}\text{Sm}$  disappears. For such weak peaks, though, such a procedure leaves a large uncertainty about any actual remaining intensity.

The coincidence data are therefore essential. The  $\gamma\gamma$  coincidence spectra show weak evidence for a possible 401 keV peak in coincidence with transitions of 444, 494, 644, and 671 keV known to feed the  $2_3^+$  level. The combined gate is shown in Fig. 3(b). As the argument in Refs. [1,2] rests on the *weakness* of the  $2_3^+ \rightarrow 0_2^+$  transition, these data provide important evidence: namely they give an upper limit on the transition  $B(E2)$  value using the known half-life of the  $2_3^+$  level [10] ( $T_{1/2} = 0.87$  ps). Our result concerning this  $B(E2)$  value can be expressed in two useful ways:

$$\frac{B(E2 : 2_3^+ \rightarrow 0_2^+)}{B(E2 : 2_3^+ \rightarrow 0_1^+)} \leq 0.015$$

and

$$B(E2 : 2_3^+ \rightarrow 0_2^+) \leq 0.05 \text{ W.u.}$$

These values are about 3.5 times *smaller* than those reported in Ref. [1] and confirm the highly forbidden nature of the  $2_3^+ \rightarrow 0_2^+$  transition, consistent with its interpretation in terms of a forbidden 2-phonon  $\rightarrow 0$ -phonon transition as discussed in Ref. [2]. Indeed, the fact that it is *smaller* than in Ref. [1] strengthens support for the coexistence argument.

The present results also resolve the puzzle of the reported 520 W.u.  $2_2^+ \rightarrow 0_2^+$  transition. We *do* observe this transition, of energy 126 keV, in the coincidence spectra, despite its proximity to the enormously intense  $2_1^+ \rightarrow 0_1^+$  transition of 121 keV. As shown in Fig. 3(c), it appears in coincidence with transitions of 275, 482, 769, and 839 keV which are known to feed the  $2_2^+$  level. We obtain an intensity branching ratio  $I(2_2^+ \rightarrow 0_2^+)/I(2_2^+ \rightarrow 2_1^+) = 0.004(1)$  that, combined with the level half-life of 7.4(6)ps [10], gives  $B(E2 : 2_2^+ \rightarrow 0_2^+) = 107(27)$  W.u. This is much lower than the existing value of 520(170) W.u., and is at least in the realm of interpretability (see below).

A third significant result concerns the 275 keV  $2_3^+ \rightarrow 2_2^+$  transition. As noted earlier, in an interpretation in which the levels above the  $0_2^+$  state are considered as a sequence of phonon excitations, this should be an allowed transition with a  $B(E2)$  value twice that for the  $2_2^+ \rightarrow 0_2^+$  transition, or 214 W.u. However, the NDS accord it an  $M1$  multipolarity based on the ratio of the electron intensity measured in Ref. [14] to the  $\gamma$ -ray intensity measured in previous studies [10] of the decay of  $^{152}\text{Eu}$ . Our  $\gamma$ - $\gamma$  measurement, shown in Fig. 3(b), however, gives a relative intensity  $I(2_3^+ \rightarrow 2_2^+)/I(2_3^+ \rightarrow 0_1^+)$

$= 0.008(1)$ , a factor of two *higher* than previously obtained. Therefore, the empirical conversion coefficient also changes by a factor of 2, from 0.105(19) to 0.046(8), and is consistent with pure  $E2$  character. The  $E2$  multipolarity and the higher intensity now give a  $B(E2 : 2_3^+ \rightarrow 2_2^+)$  value of 27(4) W.u.

For the  $4_2^+$  level, our measurements give an intensity ratio  $I(4_2^+ \rightarrow 2_2^+)/I(4_2^+ \rightarrow 4_1^+) = 0.11(1)$  [see Fig. 3(d)]. The  $B(E2 : 4_2^+ \rightarrow 4_1^+)$  value of 9 W.u. is only very roughly known [12] from an analysis of Coulomb excitation experiments. Using this value with our new branching ratio data gives a  $B(E2 : 4_2^+ \rightarrow 2_2^+)$  value of  $\sim 330$  W.u. but we stress that this is reliable only to the same rough degree as the  $B(E2 : 4_2^+ \rightarrow 4_1^+)$  value from Ref. [12].

For the  $4_3^+ \rightarrow 4_2^+$  transition, we observe no  $\gamma$  branch. However, our data give an upper limit of  $B(E2 : 4_3^+ \rightarrow 4_2^+) \leq 35$  W.u. We will see the implications of this limit below. Similarly, we obtained an upper limit of  $\leq 250$  W.u. for the  $4_3^+ \rightarrow 3_1^+$  transition.

### III. INTERPRETATION OF $^{152}\text{Sm}$

We present the full set of positive parity levels with definite spin assignments ( $J \leq 6^+$ ) and known decay below 1.5 MeV in Fig. 4. The experimental  $B(E2)$  values are indicated by the thickness of the transition arrows. The weak 401 keV  $2_3^+ \rightarrow 0_2^+$  transition, which produced the key signature in Refs. [1,2], is indicated in the figure by a dashed line of the thinnest category ( $< 5$  W.u.), but we stress that its upper limit ( $\leq 0.05$  W.u.) is actually extraordinarily weak. For the  $3_1^+$  and  $2_4^+$  levels only upper limits on  $T_{1/2}$  are known. Therefore, the  $B(E2)$  values from these levels are lower limits only as the notation in Fig. 4 indicates. For these levels, and for the  $6_2^+$  level for which no lifetime is known, the relative branching ratio data are more significant. These are discussed further below.

In order to focus on the facets of the  $^{152}\text{Sm}$  level scheme that most affect its interpretation we show in Fig. 5 (left) a number of key empirical results relating to the possible coexisting vibrational structure of the  $0_2^+$ -based levels. In the middle are predictions of the vibrator model itself for the  $0_2^+$ -based levels: the  $B(E2)$  values are obtained by normalizing to the  $2_2^+ \rightarrow 0_2^+$  1-phonon to ‘‘ground state’’ transition strength of 107 W.u. On the right are predictions of the IBA which we will discuss later.

We see immediately, by comparison with Fig. 2, that the new results have a significant effect on the understanding of  $^{152}\text{Sm}$  and resolve some of the puzzles we enumerated earlier. First, we established a more stringent (weaker) limit on the  $2_3^+ \rightarrow 0_2^+$  transition. Secondly, the  $B(E2 : 2_2^+ \rightarrow 0_2^+)$  value of 107 W.u. is much more plausible than the previous value of 520 W.u. Thirdly, the  $2_3^+ \rightarrow 2_2^+$  transition is now  $E2$  (rather than  $M1$ ), and has 27 W.u. Finally, the  $4_3^+ \rightarrow 4_2^+$  transition is found to be no more than 35 W.u.

We have noted that several aspects of the  $^{152}\text{Sm}$  level scheme seem to point to a picture of coexisting deformed or near deformed yrast states and vibrational levels built on the

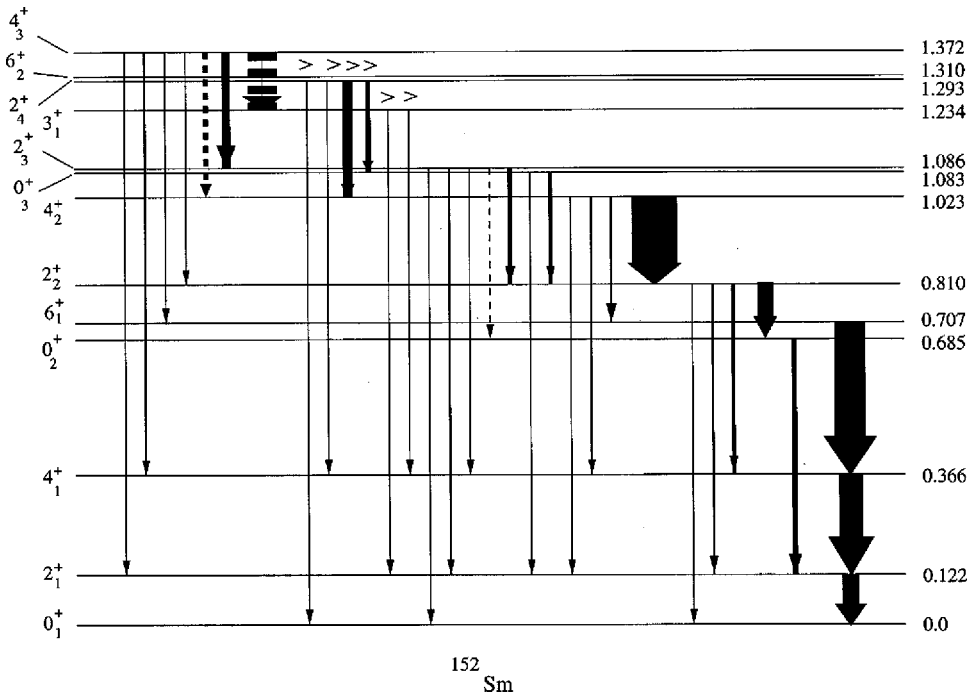


FIG. 4. Levels and transitions in  $^{152}\text{Sm}$  including the new results from the present work.  $B(E2)$  values are approximately indicated by the different thickness categories of the transition arrows. For the  $3_1^+$  and  $2_4^+$  levels, the relative  $B(E2)$  values of the transitions indicated were measured but only upper limits on the level lifetimes are known. Hence the symbol ">" indicates that these  $B(E2)$  values (arrow thicknesses) are lower limits. Dashed arrows from the  $2_3^+$  and  $4_3^+$  levels stem from upper limits on the transition intensities. Here and in Fig. 6, some level energy differences differ from their connecting  $\gamma$ -ray energies cited in the text due to rounding.

$0_2^+$ -state. The fuller level scheme in Fig. 4 gives further details that support this, in particular, the branching ratios for the  $2_2^+$ ,  $4_2^+$ ,  $2_3^+$ , and  $2_4^+$  levels that favor the  $0_2^+$ -based levels over the yrast states and that favor 1-phonon changing transitions over 2-phonon changing ones.

However, as shown in Fig. 5, there are still several very large and important discrepancies that preclude a simple harmonic vibrator interpretation. Specifically, while the  $2_2^+ \rightarrow 0_2^+$  transition (107 W.u.) is much weaker than the earlier

data it is still almost as large as the yrast  $2_1^+ \rightarrow 0_1^+$   $B(E2)$  value of 144 W.u., which is surprising if the  $0_2^+$ -based levels are supposed to be less collective vibrational levels. In a similar vein, the  $2_2^+ - 0_2^+$  energy spacing is comparable to the deformed yrast  $2_1^+ - 0_1^+$  spacing. The  $2_3^+ \rightarrow 2_2^+$  transition, though now E2, is still nearly an order of magnitude weaker than predicted by the vibrator. The same is true of both transitions from the  $4_3^+$  level. Finally, there are crossover transitions to the yrast levels [ $0_2^+ \rightarrow 2_1^+$  and  $2_2^+ \rightarrow 4_1^+$ ] that are as

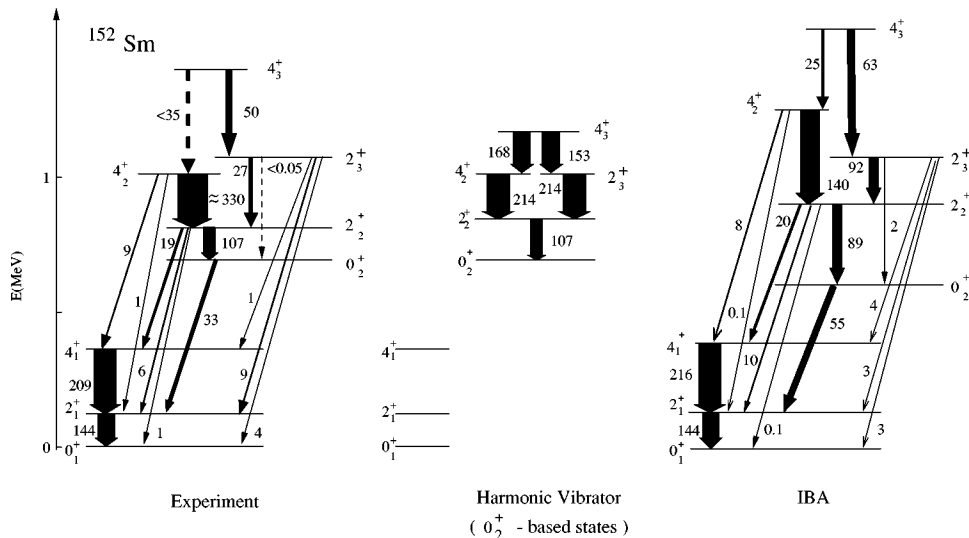


FIG. 5. Summary of key experimental energies and absolute  $B(E2)$  values (or limits) in  $^{152}\text{Sm}$  (left). Numbers on the transition arrows are  $B(E2)$  values in W.u. Dotted arrows denote upper limits. These results are compared with the predictions of the harmonic vibrator model (in the middle panel) applied to the states built on the  $0_2^+$  level. In this panel, the  $B(E2 : 2_2^+ \rightarrow 0_2^+)$ , or 1-phonon to 0-phonon, value is normalized to the new experimental result of 107 W.u. The right panel gives the predictions of the IBA (with parameters  $\epsilon/\kappa=30$  and  $\chi = -\sqrt{7}/2$ ). To avoid clutter in the experimental and IBA panels the crossover transitions from the  $4_3^+$  level to the yrast states are not shown. In all cases, in both the data and the IBA, they are weak ( $\leq 9$  W.u.). Vertical arrows denote transitions within either the yrast band or within the family of states built on the  $0_2^+$  level. Slanted arrows are crossover transitions between these two families of levels.

collective as the  $2_3^+ \rightarrow 2_2^+$  and  $4_3^+ \rightarrow 4_2^+$  transitions, while other crossover transitions are extremely weak.

We will approach an interpretation of the data in two alternate ways, by an essentially model independent, but multiparameter, mixing calculation and by a detailed IBA calculation with few parameters.

**A. Two-state mixing analyses of  $^{152}\text{Sm}$**

Before we discuss the coexistence interpretation in more detail we address the question of whether alternate interpretations are viable and, in particular, if the data can be interpreted by mixing of various states. One possible scenario could be that *all* the levels of  $^{152}\text{Sm}$  are rotational and that the properties of the  $0_2^+$ -band sequence [low  $R_{4/2}^{(2)}$  value, some collective “ $0_2^+ \rightarrow$  yrast”  $B(E2)$  values] are due to mixing effects. In this traditional view, the low-lying levels of  $^{152}\text{Sm}$  comprise the familiar ground,  $\beta$ , and  $\gamma$  bands. One obvious problem with such an interpretation would be the spacing of levels in the supposed  $\beta$  band, where, for example, the  $R_{4/2}^{(2)}$  ratio is only 2.69, far from the rotor value of 3.33. We therefore ask if it is possible to account for the observed  $R_{4/2}^{(1)}$  and  $R_{4/2}^{(2)}$  values by starting with two  $K=0$  level sequences closer to the rotor value of 3.33 and allowing for mixing. For mixing between the  $0_1^+ - 0_2^+$ ,  $2_1^+ - 2_2^+$ , and  $4_1^+ - 4_2^+$  levels, the answer is trivially negative. Such  $\Delta K=0$  mixing in the rotor has an inherent spin dependence  $V(J) \sim \sqrt{J(J+1)} \approx J$  and therefore *increases* with spin  $J$ . Therefore it can only *compress* the yrast levels and expand the  $0_2^+$  family leading to a larger (not a smaller) perturbed  $R_{4/2}^{(2)}$  value for the latter.

Another conceivable scenario would start with two intermediate  $R_{4/2}$  values near, say, 2.85, and test if mixing could result in the observed ratios of 3.01 and 2.69. We have carried out such calculations and can only reproduce the observed energies and  $B(E2)$  values by assuming unrealistic initial conditions such as very large interband  $B(E2)$  values (e.g.,  $0_2^+ \rightarrow 2_1^+$ ) or inconsistent combinations of intraband energies and  $B(E2)$  values.

In principle, it might be possible to account for the data for the “ $0_2^+$ -yrast” levels by mixing a rotational sequence

based on the  $0_2^+$  state with higher-lying states [e.g.,  $2_3^+$ ,  $4_3^+$ ], which could compress the unperturbed  $K=0_2^+$  band, in such a way as to lower  $R_{4/2}^{(2)}$ . However, one again finds that the  $J$  dependence of band mixing matrix elements in a deformed nucleus does not allow a consistent solution. Moreover, Riedinger *et al.* [15] carried out both 2- and 3-band mixing calculations and showed that one cannot consistently account for the  $B(E2)$  values from the  $0_2^+$ ,  $2_2^+$ , and  $4_2^+$  levels in this way. Indeed, many years ago, Mottelson [16] pointed out the difficulty with a rotational picture for  $^{152}\text{Sm}$ , noting especially the large  $B(E2 : 2_2^+ \rightarrow 2_1^+)$  value. Data on the decay of the  $0_2^+$ -based states obtained since Ref. [15] do not alter this conclusion. Moreover, such bandmixing cannot at all account for the energies of the “ $0_2^+$ -yrast” states. If mixing with a  $\gamma$ -band-like structure is done in order to specifically fit these observed energies and the  $R_{4/2}^{(2)}$  value [rather than the  $B(E2)$  values as in Ref. [15]], then, when carried to higher spins, the large mixing matrix elements required would lead to initial, unperturbed  $\gamma$ -band energies that are not even monotonic in  $J$  (e.g.,  $8_\gamma^+$  below  $7_\gamma^+$ ). Finally, such mixing, or mixing with still higher levels such as the  $2_4^+$  state, cannot be invoked because it would lead to strong  $2_3^+ \rightarrow 0_2^+$  or  $2_4^+ \rightarrow 0_2^+$   $B(E2)$  values. But, the former transition (401 keV) is precisely the one whose small value ( $\ll 1$  W.u.) initiated the discussion [1,2] of phase coexistence in  $^{152}\text{Sm}$ , and the latter has not been observed. Thus, mixing with higher rotational levels cannot explain the sequence of states above the  $0_2^+$  level.

We therefore return to the coexistence picture and ask if we can account for the empirical results by starting with near-rotor and near-vibrator levels and allowing mixing between them. One experimental fact greatly simplifies the calculations: Most of the transitions from the  $0_2^+$ -“non-yrast” levels (e.g.,  $2_3^+$ ,  $0_3^+$ , ...) to the ground band levels are weak. For example,  $B(E2 : 2_3^+ \rightarrow 0_1^+) = 3.6$  W.u.,  $B(E2 : 0_3^+ \rightarrow 2_1^+) = 0.8$  W.u., and  $B(E2 : 2_3^+ \rightarrow 4_1^+) = 0.8$  W.u. This effectively rules out any substantial mixing *except* for the mixing of the ground state band levels with the “ $0_2^+$ -yrast” levels. This in turn means that we can do a simple 2-state mixing analysis.

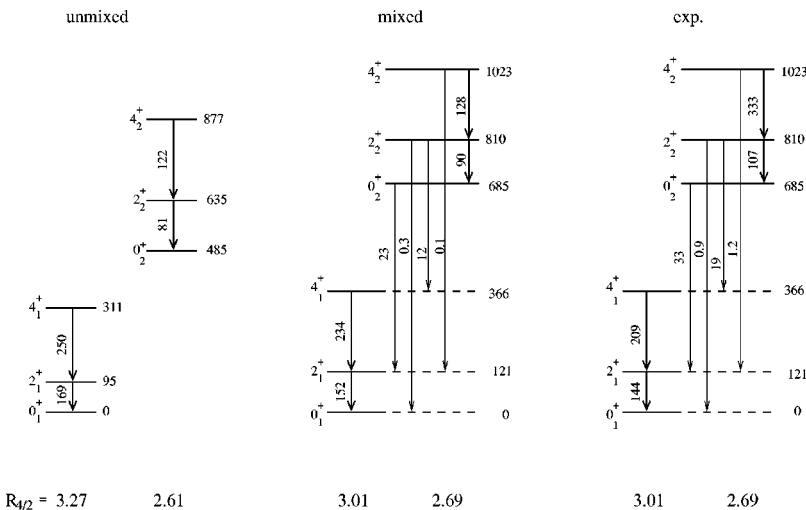


FIG. 6. Results of the mixing calculations. Left: Unperturbed energy levels and  $B(E2)$  values (in W.u.). Middle: the perturbed values resulting from the mixing matrix elements in Table II. Right: the experimental level scheme.

For the  $0_1^+ - 0_2^+$ ,  $2_1^+ - 2_2^+$ , and  $4_1^+ - 4_2^+$  level pairs we have three unknown mixing amplitudes and we want to see if the mixing can reproduce the known  $B(E2)$  values connecting these levels as well as the final (perturbed) energies.

By assuming unperturbed  $B(E2)$  values of  $B(E2 : 2_1^+ \rightarrow 0_1^+) = 169$  W.u. and  $B(E2 : 2_2^+ \rightarrow 0_2^+) = 81$  W.u. we obtain the solution shown in Fig. 6. These unperturbed  $B(E2)$  values are reasonable for rotor and vibrator sequences in a nucleus with  $N_p N_n = 96$ : a typical saturation value for the rotor is the  $B(E2 : 2_1^+ \rightarrow 0_1^+)$  value of 250 W.u. in  $^{166}\text{Dy}$  with  $N_p N_n = 288$  and a typical vibrator nucleus  $^{114}\text{Cd}$  with  $N_p N_n = 32$  has  $B(E2 : 2_1^+ \rightarrow 0_1^+) = 31$  W.u.

The mixing matrix elements and mixing amplitudes in these calculations are summarized in Table II. The solution requires mixing matrix elements of 240, 216, and 180 keV for the  $0^+$ ,  $2^+$ , and  $4^+$  levels, respectively, and results in squared mixing amplitudes for the  $0^+$ ,  $2^+$ , and  $4^+$  states that vary systematically from 0.15 to 0.11 to 0.06, respectively. The matrix elements are of the same order as those found [17] in the  $A \sim 100$  and 190 regions ( $\sim 120$  and 85 keV, respectively) for mixing of the yrast levels with intruder states from the next major shell. Since the states in  $^{152}\text{Sm}$  all stem from the same major shell, it is not surprising that their mixing is somewhat larger.

The mixing shown in Fig. 6 gives perturbed  $2_1^+ \rightarrow 0_1^+$  and  $2_2^+ \rightarrow 0_2^+$  transitions close to the observed values as well as crossover  $B(E2)$  values (both moderately collective and weak ones) that agree with experiment. These results support the idea of admixed coexisting spherical and deformed states since the needed initial unperturbed  $E(4^+)/E(2^+)$  ratio  $R_{4/2}^{(1)}$  (unperturbed) = 3.27 is very close to the rotor limit and  $R_{4/2}^{(2)}$  (unperturbed) = 2.61 is well within the anharmonic vibrator range. Moreover, the unperturbed  $0^+ - 2^+$  spacing is 95 keV for the yrast levels and 150 keV for the  $0_2^+$  sequence. The former is reasonable for near-rotational levels in this mass region. The latter, though significantly larger than for the rotational yrast states, as would be expected for a vibrational structure, is somewhat smaller than typical vibrational energies. This is, perhaps, related to the width of the potential.

Thus, we see that, with reasonable mixing matrix elements and the resulting mixing amplitudes, the seemingly large (for a vibrator)  $2_2^+ \rightarrow 0_2^+$   $B(E2)$  value, fairly large crossover  $B(E2 : 0_2^+ \rightarrow 2_1^+)$  and  $B(E2 : 2_2^+ \rightarrow 4_1^+)$  values, weak values for other crossover  $B(E2)$  values, and the nearly equal  $0^+ - 2^+$  spacings in the two level groups (121 and 126 keV, respectively) can be accounted for. Moreover, in support of the coexistence picture, the sequence of unperturbed levels built on the  $0_2^+$  state is significantly more vibrational than the unperturbed yrast levels. We will also see that this mixing analysis is consistent with the IBA treatment to be described next.

This mixing calculation should be understood in the sense that it provides an existence proof that one can start with unconnected rotor and vibrator sequences of states and reasonable mixing matrix elements and reproduce the experimental results. However, since it has a large number of parameters and invokes only 2-state mixing, it has little predictive power beyond this. We therefore turn to a more

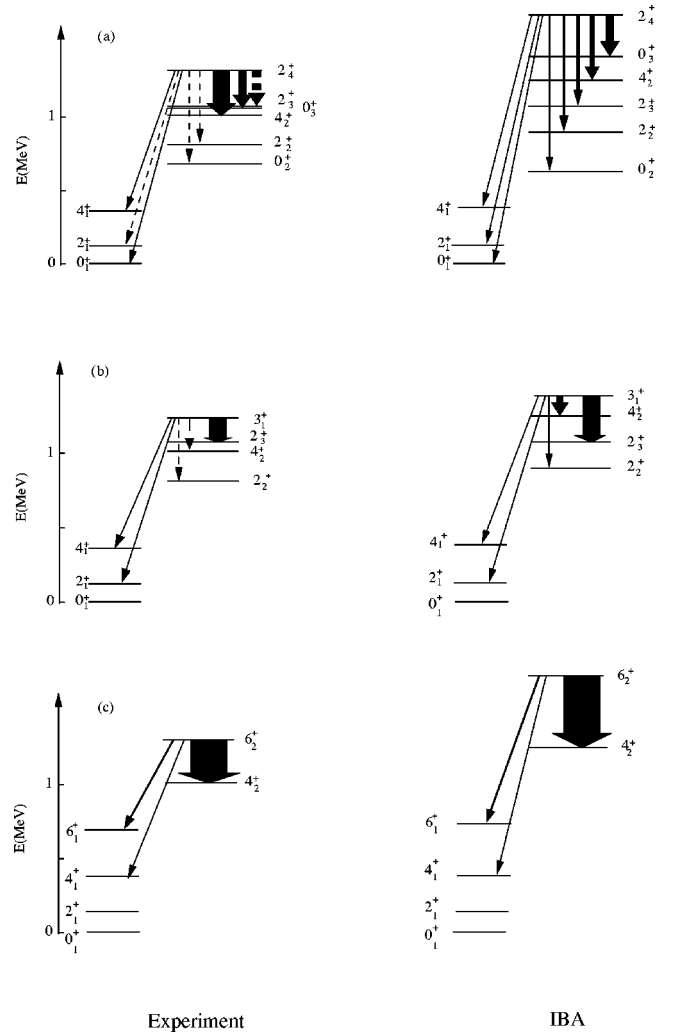


FIG. 7. Energies and relative  $B(E2)$  values for the transition from the  $2_4^+$ ,  $3_1^+$ , and  $6_2^+$  levels in  $^{152}\text{Sm}$ , compared with the IBA predictions. The thickness of the transition's arrows is a guide to the relative  $B(E2)$  values. In the experimental results, dashed lines are upper limits due either to unknown multipolarities or to unobserved transitions.

economical picture and discuss IBA calculations for  $^{152}\text{Sm}$  that give a full self-consistent set of predictions to be compared to the data.

### B. IBA calculations for $^{152}\text{Sm}$

We investigate the predictions of the IBA model for  $^{152}\text{Sm}$  with the Hamiltonian

TABLE II. Results of the 2-state mixing analysis.

$J$	Mixing matrix element $V$ (keV)	Squared $K=0^+$ mixing amplitude
0	240	0.15
2	216	0.11
4	180	0.06

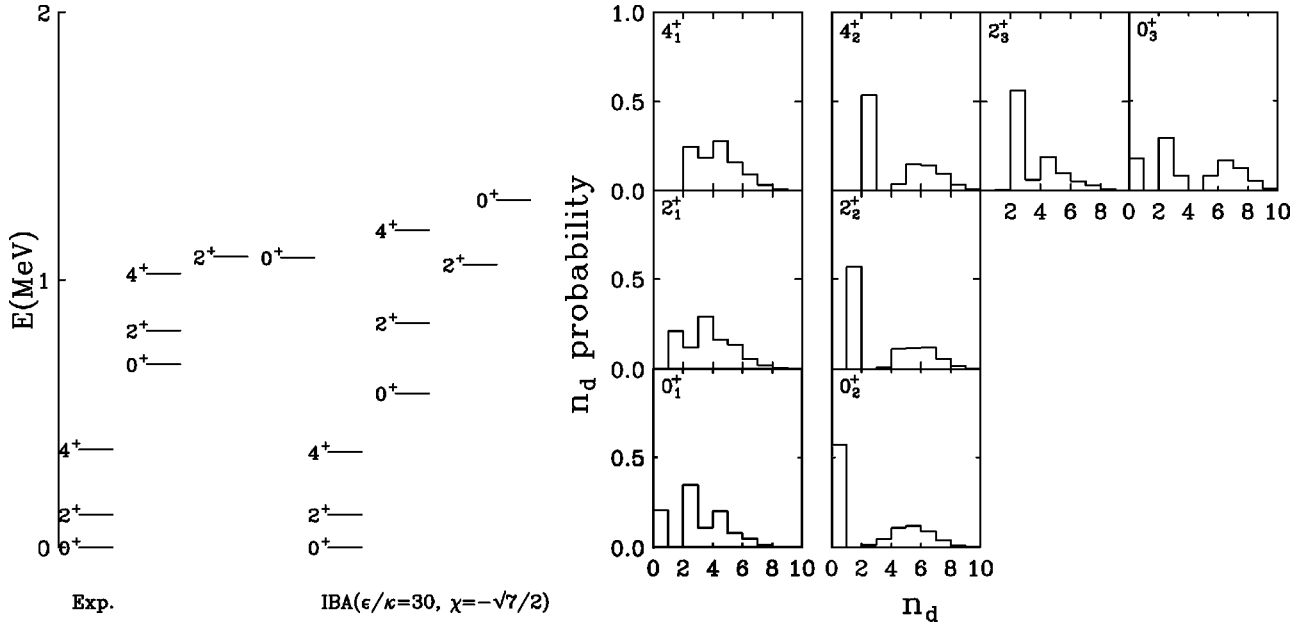


FIG. 8.  $n_d$  probability distributions for the IBA calculations ( $\epsilon/\kappa=30$  and  $\chi=-\sqrt{7}/2$ ).

$$H = \epsilon n_d - \kappa Q \cdot Q, \quad (1)$$

where  $Q = (s^\dagger \tilde{d} + d^\dagger s) + \chi (d^\dagger \tilde{d})^{(2)}$ . The parameters are  $\epsilon$ ,  $\kappa$ , and  $\chi$ , and the boson number for  $^{152}\text{Sm}$  is  $N_B = 10$ . As noted in Refs. [1,2], the key branching ratio that provides the signature of phase coexistence, namely  $R_{og}^\gamma \equiv B(E2 : 2_3^+ \rightarrow 0_2^+) / B(E2 : 2_3^+ \rightarrow 0_1^+)$ , is very sensitive to  $\epsilon/\kappa$  and  $\chi$ . It was shown there that only for a very small range of  $(\epsilon/\kappa, \chi)$  values are  $R_{og}^\gamma$  values  $\ll 1$  [1]. Thus, the parameters of Eq. (1) are highly constrained by the low empirical value  $R_{og}^\gamma \leq 0.015$ .

This small value occurs because of the near vanishing of the  $2_3^+ \rightarrow 0_2^+$   $B(E2)$  value, which is  $\leq 0.05$  W.u. Of course,  $B(E2)$  values that are such a small fraction of a W.u. can always arise from tiny amplitudes in the wave function that are beyond the scope of any existing model. Therefore, it is pointless to demand that the calculations (which only include collective degrees of freedom) give  $B(E2 : 2_3^+ \rightarrow 0_2^+)$  values as small as the data. What is essential, though, is that the calculations give predictions for this  $B(E2)$  value that are much less than typical collective magnitudes ( $\sim 10 - \sim 100$  W.u.) in  $^{152}\text{Sm}$ .

It also turns out that most of the other predictions of  $B(E2)$  values or energies are *not* very sensitive to  $(\epsilon/\kappa, \chi)$  values, *provided* the latter are in the range that produces small values of  $R_{og}^\gamma$ . A reasonable choice of  $(\epsilon/\kappa, \chi)$  is actually that used by Scholten *et al.* [18], namely

$$(\epsilon/\kappa, \chi) = \left( 30, -\frac{\sqrt{7}}{2} \right).$$

The results of the IBA calculation for these parameters are shown on the right in Fig. 5 and in Fig. 7. Figures 8 and 9 give interpretations of the structure of the IBA wave functions. These calculations are nearly the same as those of Ref.

[18] except that we have dropped the  $L \cdot L$  term in the Hamiltonian and we show predictions for a larger number of observables.

Generally speaking, the overall agreement with the data is quite good. The yrast  $B(E2)$  values are well reproduced as are the characteristic deexcitation patterns for the higher states. The energies are in reasonable agreement with the data although the spacings amongst the higher levels in the calculations tend to be larger than observed.

To consider these results in more detail, we first discuss Fig. 5 where the IBA predictions on the right can be compared with both the data and the harmonic vibrator. The predicted  $B(E2)$  value for the  $2_2^+ \rightarrow 0_2^+$  transition is in good agreement with the data. The predicted  $4_2^+ \rightarrow 2_2^+$  transition is also strong as expected. It is a little weaker than found experimentally, but we recall that this experimental value is based on a branching ratio (see Table I) involving the poorly known value of the  $B(E2 : 4_2^+ \rightarrow 4_1^+)$  value. Of course, the  $2_3^+ \rightarrow 0_2^+$  transition is weak since the near vanishing of this transition was the key to selecting the IBA parameters to begin with. Indeed, this transition vanishes for  $\epsilon/\kappa \sim 25$  [1] and remains small for the  $\epsilon/\kappa = 30$  ratio we use here.

Therefore, more interesting, and remarkable, are a series of predictions for other transitions from this and higher levels, especially for the collective transitions that, though remaining collective, are significantly changed from the harmonic vibrator predictions. The  $2_3^+ \rightarrow 2_2^+$  transition, for example, is reduced to well under half the harmonic vibrator value in better agreement with the data although it is still significantly larger than the measured value. Another interesting case (see Fig. 4) is the decay of the  $0_3^+$  state to the  $2_2^+$  level. In the harmonic vibrator this transition should have 214 W.u. whereas experimentally it is only 22 W.u. The IBA calculation again leads to a strong reduction in this  $B(E2)$  value, to 103 W.u., although the calculated value still exceeds the experimental one by a significant amount.



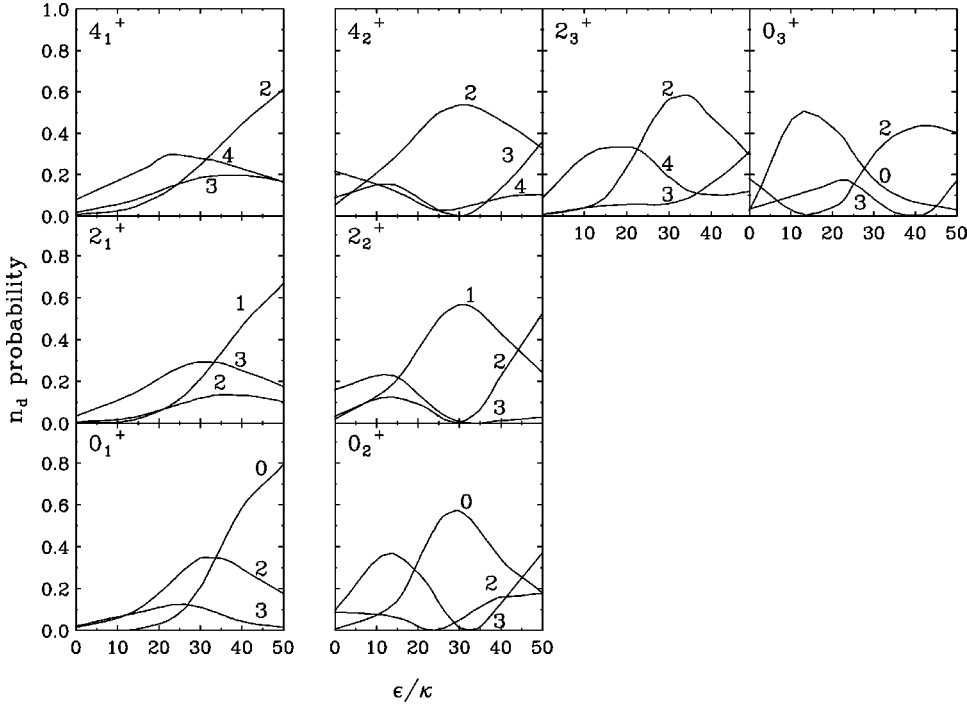


FIG. 9. Evolution of wave function probabilities with specific  $n_d$  values for IBA calculations as a function of  $\epsilon/\kappa$  ( $N_B = 10$ ,  $\chi = -\sqrt{7}/2$ ). The numbers on each curve give the corresponding  $n_d$  values. Only major  $n_d$  components are shown.

Another important case where the IBA predictions differ significantly from the vibrator concerns the  $4_3^+$  level. The predicted decay of this state is completely consistent with the data. The IBA calculation reproduces the facts that the collective  $B(E2)$  values from this level are a small fraction of the vibrator values and that crossover transitions and transitions forbidden in the vibrator are weak. We will return to the results for the  $2_3^+$ ,  $4_3^+$ , and  $0_3^+$  states momentarily.

No lifetimes are known for the  $2_4^+$ ,  $6_2^+$ , and  $3_1^+$  levels. Therefore, for these, we compare relative  $B(E2)$  values with the IBA calculations in Fig. 7. Again, the agreement is rather good, with the exception of the  $2_4^+ \rightarrow 4_2^+$  transition. Allowed transitions are strong, and forbidden or crossover ones are weak.

To sum up this discussion, the IBA calculations are able to reproduce most of the observed properties of the coexisting families of states in  $^{152}\text{Sm}$ , including a number of transitions that, while collective, are at the same time sharply reduced from the values of a pure vibrator model for the  $0_2^+$ -based levels. The only notable discrepancies concern the  $2_3^+ \rightarrow 2_2^+$  and  $0_3^+ \rightarrow 2_2^+$  transitions but, even for these, the IBA is significantly better than the pure vibrator. The IBA calculations also naturally account for mixing of the deformed and spherical phases (as manifest in the crossover transitions). It is also worth commenting for completeness that a commonly discussed signature of shape coexistence is the enhancement of  $E0$  transitions [19] and that the IBA calculations reproduce the large  $\rho(E0:0_2^+ \rightarrow 0_1^+)$  value in  $^{152}\text{Sm}$  [18].

Having illustrated the comparison of the IBA calculation with the data, we can now turn to an examination of the structure of the calculated states as seen in the IBA wave functions themselves. In Ref. [2], we discussed the  $n_d$  decomposition of the IBA wave functions for  $0^+$  states

in  $^{152}\text{Sm}$ . A more extensive set is now shown in Fig. 8 along with a comparison of the experimental and theoretical energies so that the state labels in the  $n_d$  distributions can be quickly related to our discussion of coexistence. The yrast states show a broad  $n_d$  distribution typical of a deformed rotor structure. The  $0_2^+$ ,  $2_2^+$ ,  $4_2^+$ , and  $2_3^+$  states show the characteristic dominance of single  $n_d$  components that one would expect for a vibrator.

The low lying  $0_2^+$ -based states have calculated wave functions that also show the phase mixing we have discussed earlier. The broad distribution of  $n_d$  components other than the dominant vibrational component is similar to that of the lowest SU(3) states. For example, the  $0_2^+$  state is mainly a combination of a U(5)  $n_d=0$  and SU(3)  $(\lambda, \mu) = (2N, 0)$  components while the  $2_3^+$  level is roughly a linear combination of  $n_d=2$  and a  $(2N-4, 2)$  SU(3) wave function. Indeed, the weakness of the  $2_3^+ \rightarrow 0_2^+$  transition can be qualitatively understood by the approximation that the wave functions of these states are mixtures or linear combinations of single U(5) and SU(3) components. For these two states an  $E2$  transition is therefore forbidden both between the initial and final U(5) components (because  $\Delta n_d = 2$ ) and between the initial and final SU(3) components [because  $\Delta(\lambda, \mu) \neq 0$ ]. Though a proper calculation of course needs to take account of amplitudes from cross transitions between the two components and from the small residual parts of the wave functions that cannot be so simply described, this type of analysis helps in understanding the weakness of the calculated  $B(E2: 2_3^+ \rightarrow 0_2^+)$ .

Interestingly, some of the higher states are beginning to show a dissolution of simple vibrator structure. This

is evident for the  $0_3^+$  level in Fig. 8 but is also true for the  $2_4^+$  and  $4_3^+$  levels, for which the predicted collective  $B(E2)$  values are significantly lower than the pure vibrator predictions. The fact that the IBA predictions for the phonon-allowed  $2_3^+ \rightarrow 2_2^+$  and  $0_3^+ \rightarrow 2_2^+$  transitions are still larger than the data could suggest that empirically there is even greater fragmentation of the vibrator structure for these lower spin multiphonon states. Given the agreement in energies of the higher spin  $0_2^+$ -based levels with an anharmonic vibrator model as shown in Fig. 1, it would be therefore interesting to measure  $B(E2)$  values from these states to study if there is a dependence on spin of the coexisting vibrational structure.

It is also informative to see how the calculated wave functions evolve as a function of  $\epsilon/\kappa$ . These results are given in Fig. 9. They illustrate the narrow range of  $\epsilon/\kappa$  values that give a coexistence picture and the emergence of phonon structure for the levels built on the  $0_2^+$ -state as the transition region is traversed. It is only for  $\epsilon/\kappa$  values around 25–35 that a vibrator scheme above the  $0_2^+$  state is realized. The lower part of this range gives the vanishing of the  $2_3^+ \rightarrow 0_2^+$  transition [1]. The double minimum in the potential occurs near  $\epsilon/\kappa \sim 35$  [2]. Of course, what is important for the phase coexistence picture is not a second minimum *per se* but a significant flattening out of the potential as a function of  $\beta$  so that states with significantly different  $\langle\beta\rangle$  values can coexist.

Our aim in this paper has been specifically to address the issue of phase coexistence in  $^{152}\text{Sm}$ , and we have approached this question through the IBA model and its convenient  $n_d$  decomposition which clearly shows the two families of states. However, it is important to note that early calculations by Kumar [20] are also in excellent agreement with the data for  $^{152}\text{Sm}$ . It is particularly impressive that those calculations, like the IBA [18], also predate these new data. It would be interesting to look in detail at Kumar's wave functions to determine if they too show coexisting structures.

#### IV. CONCLUSIONS

To summarize, new data on  $^{152}\text{Sm}$  using the YRAST Ball array at WNSL significantly alter the interpretation of the pivotal transitional nucleus  $^{152}\text{Sm}$ . The new data show that the  $2_3^+ \rightarrow 0_2^+$  transition is even weaker than previously thought and that the  $2_2^+ \rightarrow 0_2^+$  transition has a  $B(E2)$  value of 107 (27) W.u. rather than the 520 W.u. adopted in NDS. They also reveal that the  $2_3^+ \rightarrow 2_2^+$  transition, previously thought to be  $M1$  and therefore to have a small or vanishing  $B(E2)$  value, is  $E2$ , with a moderately collective  $B(E2)$  value of 27 (4) W.u. Finally, we obtained a  $B(E2 : 4_2^+ \rightarrow 2_2^+) \sim 330$  W.u. value and established the limits that  $B(E2 : 4_3^+ \rightarrow 4_2^+) \leq 35$  W.u. and  $B(E2 : 4_3^+ - 3_1^+) \leq 250$  W.u.

The previous values of several of these transitions precluded any reasonable interpretation or successful model predictions of the extensive  $^{152}\text{Sm}$  level scheme. With the new results, the coexistence picture discussed in Ref. [2] is

strongly supported, at least for lowest levels built on the  $0_2^+$  states. A more extensive set of vibrational levels built on the  $0_2^+$  level was discussed, and the  $E2$  transitions connecting these levels with the deformed yrast levels were interpreted with a simple 2-state mixing calculation. IBA calculations show good overall agreement with nearly all of the known  $E2$  data. Both collective and forbidden transitions are well reproduced. The former transitions, though collective, are often predicted by the IBA to be much weaker than in the vibrator model and these predictions are in better agreement with the data. Nevertheless, discrepancies remain for the  $2_3^+$  and  $0_3^+$  levels, perhaps suggesting greater dissolution of vibrator structure than calculated and than for the higher spins  $0_2^+$ -based levels. The forbidden transitions belong to two classes — those forbidden in the vibrator itself (e.g., 2-phonon changing), and crossover transitions to the deformed yrast levels. The crossover transitions proceed by mixing through which some become rather collective ( $\sim 20$ – $30$  W.u.) while others remain weaker ( $< 10$  W.u.). The mixing calculations and the IBA predict both types correctly.

An analysis of the IBA wave functions shows that there is a strong (typically 50–60% probability) vibrational component in the wave functions of the  $0_2^+$ ,  $2_2^+$ ,  $4_2^+$ , and  $2_3^+$  levels. At the same time, there seems to be a dilution of a simple, strong single vibrator component in the wave functions of other  $0_2^+$ -based levels (e.g.,  $0_3^+$ ,  $2_4^+$ ,  $4_3^+$ ). This seems to be reflected in the strong reduction in their collective  $B(E2)$  values to other phonon states relative to the harmonic vibrator predictions. These reductions amount to factors of 2–10, and are in better agreement with the data than a pure vibrator, although further reduction would be necessary.

To conclude, the IBA calculations (with two parameters) reproduce the deformed yrast states, the phase coexistence, the phase mixing, the collective transitions between phonon states in the  $0_2^+$ -based vibrator levels, the weakness of 2-phonon changing transitions that are forbidden in the vibrator, the onset of dissolution of vibrational structure in some 2- and 3-phonon levels, and the varying collectivity of crossover transitions that arises from the phase mixing. Phase transitions and phase mixing in nuclei could, in principle, appear in many forms and with different characteristics. It seems that many of the specific features of phase coexistence characteristic of the IBA are in fact close to those which have now been discovered experimentally in  $^{152}\text{Sm}$ .

#### ACKNOWLEDGMENTS

We are grateful to F. Iachello, M. Riley, D.D. Warner, J. Jolie, W. Nazarewicz, D. Kusnezov, K. Heyde, and O. Scholten for significant discussions. This work was supported by the U.S. DOE under Contract Nos. DE-FG02-91ER-40609 and DE-FG02-88ER-40417.

- [1] R. F. Casten *et al.*, Phys. Rev. C **57**, R1553 (1998).
- [2] F. Iachello, N. V. Zamfir, and R. F. Casten, Phys. Rev. Lett. **81**, 1191 (1998).
- [3] R. F. Casten, D. Kusnezov, and N. V. Zamfir, Phys. Rev. Lett. **82**, 5000 (1999).
- [4] P. Debenham and N. M. Hintz, Nucl. Phys. **A195**, 385 (1972).
- [5] D. M. Brink, A. F. R. de Toledo Piza, and A. K. Kerman, Phys. Lett. **19**, 413 (1965).
- [6] M. Déléze, S. Drissi, J. Jolie, J. Kern, and J. P. Vorlet, Nucl. Phys. **A554**, 1 (1993).
- [7] R. F. Casten, J. Jolie, H. G. Börner, D. S. Brenner, N. V. Zamfir, W. T. Chou, and A. Aprahamian, Phys. Lett. B **297**, 19 (1992); **300**, 411 (1993).
- [8] A. Aprahamian, D. S. Brenner, R. F. Casten, R. L. Gill, and A. Piotrowski, Phys. Rev. Lett. **59**, 535 (1987).
- [9] J. L. Durell, in *The Spectroscopy of Heavy Nuclei*, edited by J. F. Sharpey-Schafer and L. D. Skouras, IOP Conference Series 105 (Institute of Physics, Bristol, 1990), p. 307.
- [10] Agda Artna-Cohen, Nucl. Data Sheets **79**, 1 (1996).
- [11] N. M. Stewart, E. Eid, M. S. S. El-Daghmah, and J. K. Jabber, Z. Phys. A **335**, 13 (1990).
- [12] I. A. Fraser, J. S. Greenberg, S. H. Sie, R. G. Stokstad, G. A. Burginyon, and D. A. Bromley, Phys. Rev. Lett. **23**, 1047 (1969).
- [13] C. W. Beausang *et al.* (to be published).
- [14] J. Goswamy, B. Chand, D. Mehta, N. Singh, and P. N. Trehan, Appl. Radiat. Isot. **42**, 1025 (1991).
- [15] L. L. Riedinger, H. R. Johnson, and J. H. Hamilton, Phys. Rev. **179**, 1214 (1969).
- [16] B. R. Mottelson, *Proceedings of the International Conference on Nuclear Structure*, Tokyo, 1967, edited by J. Sanada [J. Phys. Soc. Jpn. Suppl. **24**, 87 (1968)].
- [17] K. Heyde, E. D. Kirchuk, and P. Federman, Phys. Rev. C **38**, 984 (1988).
- [18] O. Scholten, F. Iachello, and A. Arima, Ann. Phys. (N.Y.) **115**, 325 (1978).
- [19] J. L. Wood, K. Heyde, W. Nazarewicz, M. Huyse, and P. van Duppen, Phys. Rep. **215**, 101 (1992).
- [20] K. Kumar, Nucl. Phys. **A231**, 189 (1974).